Journal of Applied Polymer Science

Equal-Channel Multiple Angular Extrusion of Polyethylene

Victor A. Beloshenko,[1] Andrei V. Voznyak,[1] Yuri V. Voznyak,[1] Galina V. Dudarenko[2]

[1]Donetsk Institute for Physics and Engineering named after A.A. Galkin, National Academy of Sciences of Ukraine, 72 R. Luxemburg st., 83114 Donetsk, Ukraine

[2]Institute of Macromolecular Chemistry, National Academy of Science of Ukraine, Kharkivske shausse, 48, 02160 Kyiv, Ukraine

Correspondence to: V. A. Beloshenko (E-mail: bel@hpress.fti.ac.donetsk.ua)

ABSTRACT: The effect of accumulated deformation and deformation routes in the course of equal-channel multiple angular extrusion (ECMAE) on physical and mechanical properties of polyethylene (PE) differed in molecular mass (MM) has been studied. As deformation routes, route C (shear planes are parallel, and the simple shear direction of every deformation zone is changed through 180°) and route E (shear planes are turned through ±45° around the extrusion axis and the normal to the axis, and simple shear direction is changed through 180° or ±90° with respect to the deformation zone) were selected. It has been shown that ECMAE provides the increase of microhardness H, modulus of elasticity E, and tensile strength σ_T up to 4.5 times with strain at break ε_b staying practically at the level of ε_b of the initial material. The value of the effects achieved depends on MM, accumulated deformation and the selected deformation route. The best set of physical and mechanical characteristics was observed in the case of route E. The observed effects are related to the formation of a special orientation order and increased degree of crystallinity of extrudates. According to SEM data, route C results in mostly uniaxial orientation of macrofibrils at an angle of 35° to the direction of extrusion, and formation of a part of tie fibrils and macrofibrils oriented perpendicularly to the main orientation. The route E produces biaxial orientation of macrofibrils. © 2012 Wiley Periodicals, Inc. J. Appl. Polym. Sci. 000: 000–000, 2012

KEYWORDS: polyethylene; equal-channel multiple angular extrusion; processing route

Received 23 February 2012; accepted 2 May 2012; published online
DOI: 10.1002/app.37993

INTRODUCTION

Solid-phase structure modification of polymers includes a number of methods based on plastic deformation and aimed at formation of a highly oriented state.[1] These methods include tensile stretching, uniaxial compression, rolling, drawing, plane strain compression, ram, and hydrostatic extrusion.[1,2]

The whole variety of the methods of solid-phase molecular orientation can be divided into two groups. The first group includes methods based on polymer billet deformation accompanied by form change (stretching). The second group unites processes based on simple shear not related to form and size change. The most far-famed is equal-channel angular extrusion (ECAE).[2,3]

In the course of ECAE, a billet is pressed through two channels of equal cross-sections intercepting usually at 90°. A peculiarity of ECAE is a possibility of realization of different deformation routes to generate manifold molecular orientation. They include: route A when the orientation of the billet remains the same at the every pass; route B when the billet is rotated 90° clockwise and counterclockwise alternatively around the longitudinal axis after every extrusion cycle; route C when the billet is rotated 180° around the longitudinal axis after every extrusion cycle; route D when the billet is rotated 90° clockwise around the longitudinal axis after every extrusion cycle.[3]

Only two polymer deformation routes have been studied to date: route A and C. According to Refs. 4–6, the global molecular orientation is formed in the course of polymer processing along route A. In the case of route C, local molecular orientation is created. Orientation degree is determined by the value of accumulated deformation (the number of passes through intersecting channels). Due to the structure transformation, there is an increase of modulus of elasticity and tensile strength of crystallizing polymers, as well as, in the plasticity and impact strength of amorphous polymers. However, the results listed in Refs. 7–13 do not always confirm this fact. The reason is that ECAE was carried out at room temperature, which is far from the optimum one. For instance, according to Ref. 6, extrusion temperature of 423 K is the optimum one for polyamide-6. Extrusion at lower temperatures results in the mechanical

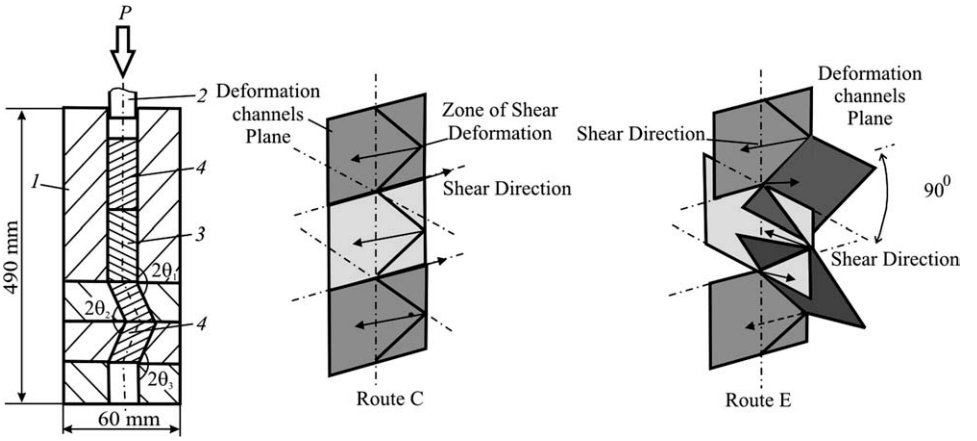

Figure 1. Scheme of ECMAE process: 1—die, 2—punch, 3—polymeric billet, 4—sacrified billets.

destruction of polymeric chains prevailing over orientation strengthening in view of limited molecular mobility. At the same time, multiple-pass ECAE at higher temperatures provides higher accumulated deformation but makes the process ineffective because of stress relaxation at cooling and the subsequent heating of the deformed polymer.

In Refs. 14–17, application possibilities of a new method of solid-phase processing based on simple shear deformation are studied, i.e., equal-channel multiple angular extrusion for structure modification of semicrystalline polymers. A peculiarity of equal-channel multiple angular extrusion (ECMAE) is that several zones of shear deformation are present within one device permitting the accumulation of high plastic deformation per one cycle. It has been shown that ECMAE does not modify the form of the initial billet but significantly increases the strength and rigidity of the tested materials and conserves high level of plasticity. At the same time, distinct from traditional solid-phase extrusion through a conic die, low anisotropy of strength properties at longitudinal and transversal sections of the processed articles is achieved through ECMAE.

The published results of Refs. 14–17 are related mostly to polyamide-6. This polymer does not allow realization of large stretching at solid-state extrusion without preliminary plasticization.[18] This fact complicates the attainment of highly oriented samples with maximum achievable deformation and strength characteristics. This problem can be eliminated by the use of polyethylene (PE) as a test subject easily amenable to solid-phase orientation.[19] In this article, three types of PE differing in the molecular mass (MM) are tested to establish the effect of the degree of plastic deformation and deformation route of ECMAE on their structure and properties.

EXPERIMENTAL

The process was implemented using a plant mounted at a hydraulic press of 1370 kN force (140t). Figure 1 demonstrates ECMAE scheme. A polymer billet is pressed through a device consisting of several pairs of channels of the same diameter intersecting at varied angles θ_i. The inlet and outlet channels were made vertically coaxial to keep the billet pointing to the right direction. Inclined channel pairs form so-called knee. Position of the knee can be changed by turning the channels around the vertical axis. The control over the position of the shearing plane in the space guarantees different variants of deformation spatial development. Figure 1 shows also the positions of deformation channels plane used in the work. They support the shear planes are parallel, and the simple shear direction of every deformation zone is changed through 180° (route C) or shear planes are turned through ±45° around the extrusion axis and the normal to the axis, and simple shear direction is changed through 180° or ±90° with respect to the deformation zone (we call it route E).

The plastic deformation intensity $\Delta\Gamma_i$ and the value of accumulated deformation ε were determined by the formula:[15]

$$\Delta\Gamma_i = 2ctg\theta_i \tag{1}$$

$$\varepsilon = 2\sum_{i=1}^{n}\frac{ctg\theta_i}{\sqrt{3}}, \tag{2}$$

where θ_i is the half-angle of channel intersection, n is the number of channel intersection angles.

Force mode of pressing was registered by pressure sensor SEN 8600 (Kobold) built-in in hydraulic cylinder. Temperature of extrusion was controlled by a thermocouple supplied on deforming channels. Temperature control and registration of extrusion pressure was done with the universal measuring controller TRM-151-01, Owen, Ukraine. Observational temperature accuracy was 0.1 K, the pressure accuracy was 1×10^{-4} MPa. The temperature of the deforming block within the container was maintained with accuracy of ±1 K. Working pressure at the plunger was estimated as:

$$P = \frac{P_1 \cdot S_1}{S_2}, \tag{3}$$

where P_1 is the reading of the built-in pressure sensor, S_1 and S_2 are the areas of cross-sections of the press and the plunger, correspondingly.

For the attaining of a uniform deformation over extrudate length and avoiding the bending of extrudate ends, we used

sacrified billets placed ahead of and behind the studied object. An incoming billet acted as the upper sacrified billet when a series of extrudates was produced.

As test subjects, high-density polyethylene CESTILENE HD500 and HD1000, QUADRANT and ultra-high-molecular-weight polyethylene (UHMWPE) were selected, that differ in the MM. Average MMs $\overline{M}_w$ were 0.5×10^6, 1.0×10^6, and 2.0×10^6, correspondingly. The billets of the required size (15 mm in diameter, 50 mm in length) were obtained by hot pressing (UHMWPE) or mechanical processing of extruded rods of 16 mm in diameter (HD500 and HD1000).

We chose the method of microhardness H measurement as one of the basic investigation methods. This allowed us not only to simplify the mechanical testing but also to obtain information on the uniformity of the strain over a section of the extrudates. Since the microhardness of polymers is proportional to the yield strength σ_y,[20] the microhardness distribution suggests the strain uniformity. Microhardness H was determined using a microhardness tester of the PMT-3 type. The indenter was a tetrahedral diamond pyramid with the vertex angle of 136°. The pyramid was fluently pressed into the sample at the loading of 0.5N. The value of microhardness H was estimated by the formula $H = 0.1854\frac{F}{d^2}$, where F—loading, N; d—diagonal of the indentation; $d^2/1.854$—area of the lateral surface of produced pyramidal indentation. For H, the relative error was not higher than 5%. The uniformity of H distribution over the sections of extrudates was estimated by value of dispersion D_H determined by the formula:

$$D_H = \sqrt{\frac{1}{n(n-1)}\sum_{i=1}^{n}(\bar{H} - H_i)^2}, \quad (4)$$

where n—number of measurements, H_i—result of an individual measurement of microhardness value, $\overline{H}$—average microhardness value. The value of microhardness anisotropy ΔH characterizing the difference in the strength properties in longitudinal and transverse sections of extrudates was estimated by the formula:[21]

$$\Delta H = 1 - \frac{\bar{H}^{\perp}}{\bar{H}^{\parallel}}, \quad (5)$$

where $\overline{H}^{\perp}$, $\overline{H}^{\parallel}$—average values of microhardness in cross and longitudinal sections of extrudates, respectively.

The dumb-bell shaped specimens (head size, diameter 10 mm; length, 10 mm; working-part size, diameter, 5 mm; length, 30 mm) were subjected to tensile tests. The specimens were cut along the direction of extrusion. The supporting platforms travelled at a velocity of 10 mm min^{-1}. The average values of yield strength σ_y, tensile strength σ_B, modulus of elasticity E, yield strain ε_y, strain at break ε_b and standard deviations were determined from testing five specimens of each sample.

The density of specimens ρ was determined by hydrostatic weighing (a balance of the AX200 type, Shimadzu Co.). The volume degree of crystallinity (χ_C^{ρ}) was calculated using the following relationship:

$$\chi_c^{\rho} = (\rho - \rho_a)/(\rho_c - \rho_a), \quad (6)$$

where ρ_a and ρ_c are the densities of polymer amorphous and crystalline phases, respectively (for PE, $\rho_a = 0.850$, $\rho_c = 1.003$ g/cm^3).[22]

The differential scanning calorimetry (DSC) was performed using a thermoanalytical complex DuPont 9900. The heating rate was equal to 20 deg/min, the weight mass—15 mg. Enthalpy of fusion, ΔH_f, was determined by integrating the area under the baseline correct thermogram. Percentage crystallinity χ_C^{DSC} was calculated from the ratio of $\Delta H_f/\Delta H_{f100\%}$, where $\Delta H_{f100\%}$ is the enthalpy of fusion for a fully crystalline polymer (for PE, $\Delta H_{f100\%} = 290$ J/g).[23]

For the determination of the thickness of crystalline stem l_c, the Gibbs-Thomson equations were used:

$$l_c = \frac{2\sigma_e T_m^0}{\Delta h_f (T_m^0 - T_m)}, \quad (7)$$

where σ_e is the lamellar basal surface free energy (for PE, $\sigma_e = 9 \times 10^{-6}$ J/cm^2,[24]), Δh_f is the heat of fusion per unit volume (for PE, $\Delta h_f = 293$ J/cm^3,[25]), T_m^0 is the equilibrium melting temperature (for PE, $T_m^0 = 418.5$ K[26]).

Scanning electron microscopy (SEM) was implemented by using a JEOL JSM-6490 instrument at an accelerating voltage of 15 kV. A conducting layer (25–30 μm—thick golden layer) was applied to surface under investigation by cathode sputtering method. The photographs were taken of the surfaces of cross and longitudinal spallings of original samples and extrudates. The spalling was made at the liquid nitrogen temperature.

MM characteristics of PE were measured with gel-chromatograph "DuPont" at 413 K in o-dichlorobenzene with the use of bimodal device "Zorbax PSM." The concentration of the polymer solution was 0.1%.

RESULTS AND DISCUSSION

The main parameters of ECMAE process are deformation intensity (the value of the angle of channel intersection), degree of accumulated deformation, temperature, rate. and pressure of extrusion.[14–17] Simple shear direction, i.e., deformation route, affects significantly the character of the formed microstructure and properties of polymers.[4–7,27,28] ECMAE with an alternating-sign deformation character realized stress-deformed material state corresponding to deformation route C or to a combination of varied deformation routes during one cycle (Figure 1).

According to data of Refs. 14, 15, the optimum conditions of PE ECMAE are $\Delta\Gamma_1 = 0.83$, the extrusion temperature of 383 K, the extrusion rate of 0.6×10^{-3} m/s. Used in the present work, these parameters allowed for the effective realization of strengthened polymer state with maximal level of mechanical properties.

Extrusion displacement dependence of ECMAE pressure is of the same character as in case of traditional solid-phase extrusion.[2] The material starts extrusion when the pressure reaches some maximum value P_m, after which the billet moves at lower

Table I. Influence of ECMAE on Microhardness of PE

Routes of deformation	Accumulated strain values	Maximum extrusion pressure, MPa	Molecular mass, $M_w \times 10^6$	Microhardness, MPa		Microhardness anisotropy	Dispersion in microhardness
				In cross section	In longitudinal section		
Initial	0		0.5	36	38	0.06	0.35
			1.0	30	32	0.06	0.43
			2.0	46	48	0.04	1.50
Route C	4.4	410	0.5	120	142	0.16	1.59
		470	1.0	94	113	0.17	1.76
		530	2.0	52	57	0.09	0.87
	6.7	500	0.5	136	160	0.15	1.03
		554	1.0	96	118	0.18	1.04
	9.1	580	0.5	152	175	0.13	1.01
		590	1.0	105	124	0.15	1.02
		680	2.0	58	62	0.07	0.77
Route E	4.4	390	0.5	150	166	0.10	1.17
		410	1.0	120	135	0.11	1.19
		500	2.0	60	64	0.06	0.80
	6.7	470	0.5	164	180	0.09	1.00
		485	1.0	125	141	0.11	1.03
	9.1	565	0.5	174	189	0.08	0.94
		580	1.0	137	150	0.09	0.98

constant pressure. The observed reduction of extrusion pressure may be attributed to a strain softening phenomenon in polymers, to the self-heating effect, or both.[9,29] Maximum extrusion pressure increases with ε growth (Table I). At equal ε, absolute values of P_m in case of route C exceed those of route E. Such a difference can be related to Bauschinger's effect,[30] that is the reduction of plastic deformation resistance at alternating-sign loading determined by the presence of residual stresses. The residual stresses together with working stress at sign alternation result in loading reduction. At that, the effect is significantly weakened at multiple cycle loadings. Bauschinger's effect will probably be stronger in the case of route E, which realizes alternating-sign deformation at different planes. The character of MM effect on the accumulated deformation ε dependence of P_m is in agreement with behavior established earlier for solid-phase extrusion through a conic die:[31] PE with lower MM requires application of lower pressure at the same ε.

Table I lists the average microhardness at longitudinal $\overline{H}^{\parallel}$ and transversal $\overline{H}^{\perp}$ sections of extrudates, the anisotropy of microhardness ΔH, and microhardness dispersion D_H at cross-section of PE samples obtained at varied deformation routes. ECMAE increases microhardness of both the sections. According to Ref. 20, the increase of microhardness of crystalline polymers is related to a higher degree of crystallinity of polymers and/or formation of orientation order. The last factor also determines the anisotropy of microhardness phenomenon ΔH. In the case of ECMAE, ΔH is reduced as the accumulated deformation ε increases. Such behavior of ΔH differs from the traditional variant of solid-phase extrusion, e.g., extrusion through a conical die, when ΔH increases with ε rising.[16] This fact is determined by the alternating-sign character of deformation at ECMAE that forms mainly microscopic molecular orientation within the extrudate.[17] It should be noted that absolute values of ΔH in the case of die extrusion significantly exceed those after ECMAE even at lower ε.[17]

The higher the value of ε is and the lower MM, the larger the increment of H. The largest value of PE microhardness is achieved at accumulated deformation ε equal to 9.1. Microhardness of extruded UHMWPE is increased in 1.5 times, HD1000 demonstrates an increase in four times, and HD500 yields an increase in six times. The succeeding increase of ε is inexpedient because of sharp (up to 1000 MPa) enhancement of extrusion pressure. The use of route E compared to route C at the same value of accumulated deformation provides higher absolute values of microhardness and lower anisotropy. At the same time, more homogeneous microhardness distribution at extrudate cross-section is achieved. In the case of HD500 and HD1000, the value of extrudate microhardness dispersion D_H exceeds that of the initial polymers but approaches its value with rising ε. D_H of initial UHMWPE is high enough and can be related to the features of its production. After ECMAE, reduction of D_H is observed, which is less essential in the case of HD500 and HD1000.

Together with increased microhardness, ECMAE provides noticeable increment in the density ρ, elastic and strength characteristics of polymers: modulus of elasticity E, yield strength σ_y, and tensile strength σ_T measured at stretching of samples cut off along the extrusion direction (Table II). Plasticity (yield strain ε_y and strain at break ε_b) becomes a bit lower. The achieved effect is determined by accumulated deformation, deformation route and MM.

Table II. Influence of ECMAE on Physical and Mechanical Properties of PE

Routes of deformation	Accumulated strain values	Molecular mass, $M_w \times 10^6$	Density, g/cm^3	Modulus of elasticity, MPa	Yield strength, MPa	Tensile strength, MPa	Yield strain, %	Strain at break, %
Initial	0	0.5	0.966	400	25	28	35.0	650
		1.0	0.962	220	20	22	30.0	520
		2.0	0.942	690	35	38	3.5	12.6
Route C	6.7	0.5	0.971	1200	87	90	34.0	605
		1.0	0.970	625	60	64	24.0	450
	9.1	0.5	0.974	1350	92	95	34.0	600
		1.0	0.970	690	62	65	24.0	448
		2.0	0.950	900	49	54	3.2	11.5
Route E	6.7	0.5	0.980	1680	112	115	34.2	620
		1.0	0.976	870	84	88	24.4	480
	9.1	0.5	0.986	1870	120	122	34.6	625
		1.0	0.980	950	90	95	24.6	505
		2.0	0.952	1080	55	59	3.3	11.9

The increase of accumulated deformation ε results in increase of E, σ_y, σ_T, that is more noticeable in the case of PE with lower MM. With increasing ε, the increase in the mentioned properties becomes slower. This phenomenon is characteristic of ECMAE of semicrystalline polymers,[15,17] differing from such methods of solid-phase processing as die-drawn, hydrostatic extrusion, and rolling, where almost linear growth of these characteristics takes place with increase in the accumulated deformation up to limiting values of the deformation degree.[32–34] It should be noted that in contrast to traditional methods of solid-phase extrusion aimed at creation of high-modulus states of crystallizing polymers, ECMAE determines balanced increase in modulus and strength. At that, the values of elastic and strength characteristics of PE with ultra-high MM ($\overline{M}_w = 2 \times 10^6$) are increased insignificantly after ECMAE, whereas PE with lower MM ($\overline{M}_w = 0.5 \times 10^6$ and 1×10^6) demonstrates the increase in several times. This fact is explained by competition of strengthening processes determined by oriented structure formation and softening caused by destruction of macromolecular chains.[35]

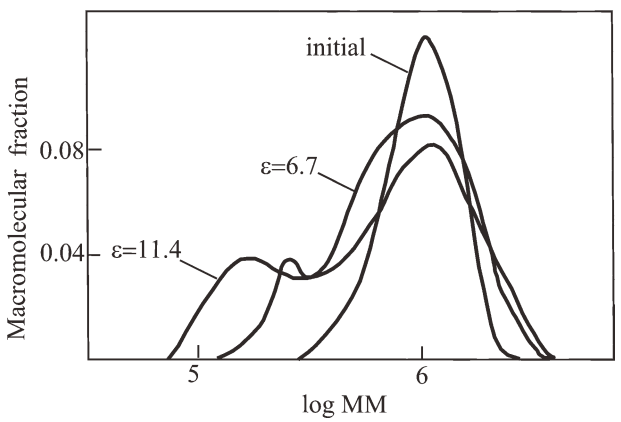

Figure 2. Differential curves of MMD of the initial HD1000 and one after ECMAE, route C.

Figure 2 presents examples of the molecular mass distribution (MMD) curves of the initial HD1000 and those after ECMAE that confirm mechanodestruction determined by deformation. The MMD curve of the initial PE is of unimodal form. ECMAE results in bimodal MM distribution. A low-polymeric peak emerges that is shifted toward lower MM with accumulated deformation increase, MMD curves widen at the rate of low-polymeric fraction formation, their polydispersity increases (Table III). As in HD500 and HD1000, orientation of macromolecular chains in the course of extrusion prevails over their destruction, a significant increase in deformation and strength characteristics occur. At maximum MM (for instance, UHMWPE), stretching of chains is limited by connecting entanglements and tie molecules that are broken at deformation. As a result, insignificant increase in rigidity and strength of extrudates is observed.

The behavior of plastic characteristics in the case of ECMAE differs from the observed one when traditional schemes of solid-phase extrusion with typical continuous reduction of plasticity with increase in accumulated deformation.[17,34,36] In the case of ECMAE, starting from definite ε, values ε_y and ε_b become constant. The best combination of elastic, strength and plastic characteristics is achieved by route E. Compared to route C, the better set of deformation-strength characteristics is formed at lower ε. Extrudate density ρ correlates to the

Table III. Influence of ECMAE (route C) on the Molecular Characteristics of HD 1000

Accumulated strain values	M_w	M_n	M_w/M_n	M_z
0	1,026,000	8,93,000	1.15	1,153,000
6.7	8,65,000	4,31,000	2.01	1,280,000
11.4	8,60,000	3,74,000	2.30	1,103,000

Table IV. Influence of ECMAE on the Structural and Thermophysical Characteristics of HD 1000

Routes of deformation	Accumulated strain values	Temperature of melting peak, T_m, K		Enthalpy of fusion, J/g	Degree of crystallinity, χ_c, from		Crystalline stem thickness, l_c, nm
		T_{m1}	T_{m2}		DSC	Density	
Initial	0	403		182	0.63	0.75	16
Route C	9.1	407	409	215	0.74	0.80	27
Route E	9.1	409	411	226	0.78	0.87	34

evolution of strength characteristics. The maximum growth is achieved at route E (Table II).

The increase in microhardness and strength characteristics of extruded PE is determined by both formation of oriented structure and enhanced degree of crystallinity of the samples.[37] The last fact is confirmed by calculation of crystallinity degree using density measurements and DSC (Table IV). DSC curves of PE extrudates indicate an increase in onset temperature, shift of the main melting peak toward higher temperatures and emergence of additional high-temperature melting peak (Figure 3). In the case of route E, melting peaks are located at higher temperatures and have areas bigger of those of samples deformed by route C. This temperature behavior can be related to destruction caused by deformation of thin crystallites and conserved or increased fraction of large crystallites due to crystallization induced by deformation. The last fact is confirmed by gain in total ennthalpy of fusion ΔH_f (Table IV). The origination of analogous melting doublet at DSC curves was noticed in Refs. 33, 38, 39 being related to formation of two types of crystal structures which differ in the degree of crystallite perfection.

The reduction of peak width observed in the case of PE samples subjected to ECMAE can be determined by decrease in dispersion of crystallite width. At the same time, partial increase in the thickness of crystalline stem l_c takes place (Table IV). The highest values of l_c are achieved after processing by route E. One can notice a small, systematic deviation of the density-based degree of crystallinity toward higher values as compared with respective values estimated from DSC data. Similar differences of crystallinity estimated from the heat of melting and density are frequently observed for many semicrystalline polymers.[40]

Figure 4 presents images of the brittle fracture surface of the initial HD1000 and subjected to the ECMAE process. The initial polymer has uniaxial spherulitic structure [Figure 4(a)]. ECMAE results in uniaxial (route C) or biaxial (route E) stretching [Figure 4(b,c)]. The scheme is presented in Figure 4(d–f). Inside the spherulite volume, rearrangement of lamellae into macrofibrils takes place. In the case of route C, macrofibrils are formed mostly at an angle close to 35° to the extrusion direction; at the same time, some part of macrofibrils is directed normally to the main orientation [Figure 5(a)]. In the case of route E, biaxial orientation of macrofibrils is formed [Figure 5(b)]. Analogous structure reconstruction is also observed in the case of HD500. The only difference is that cross-sizes of macrofibrils are smaller than those of HD1000.

It is known that after solid-phase extrusion,[34] when the process of rearrangement of the initial structure into a macrofibrillar structure finishes, further plasticity of extrudates depends on the degree of orientation of polymeric chains, structure of interfibrillar spaces, (i.e., by connectivity and density of packing of fibrillar structural units) and ability of all fibrillar morphological units to slip along one another. The last phenomenon is accompanied by intracrystalline slip, migration of defects through crystallites, an increase in orientation of molecular segments in disordered intra- and inter-fibrillar regions and increasing amount of taut tie molecules.

In the case of route E, realization of these processes without development of a main crack (i.e., conservation of plasticity of extrudates) is probably determined by formation of biaxial orientation of macrofibrils and defect boundaries (Figure 6) that restrain crack evolution. The last fact is provided for by formation of more perfect crystallites (according to DSC data) and ejection of various conformational defects (like chain ends, loops, trapped entanglements, tie molecules etc.) into the intra- or inter-fibrillar space because there is not enough free volume

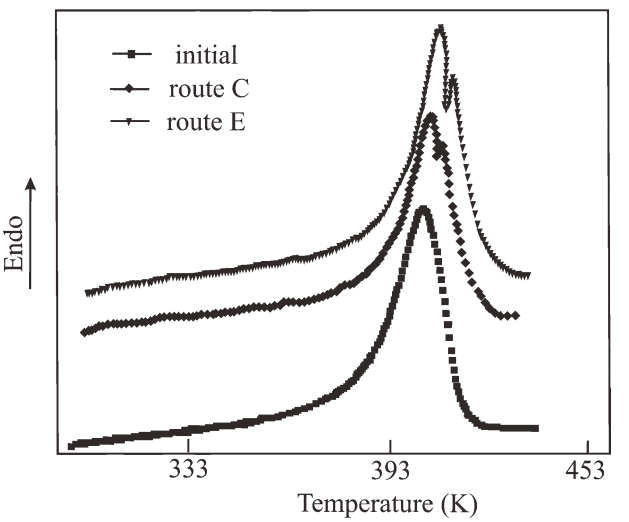

Figure 3. DSC traces for specimens of initial HD1000 and after different ECMAE routes.

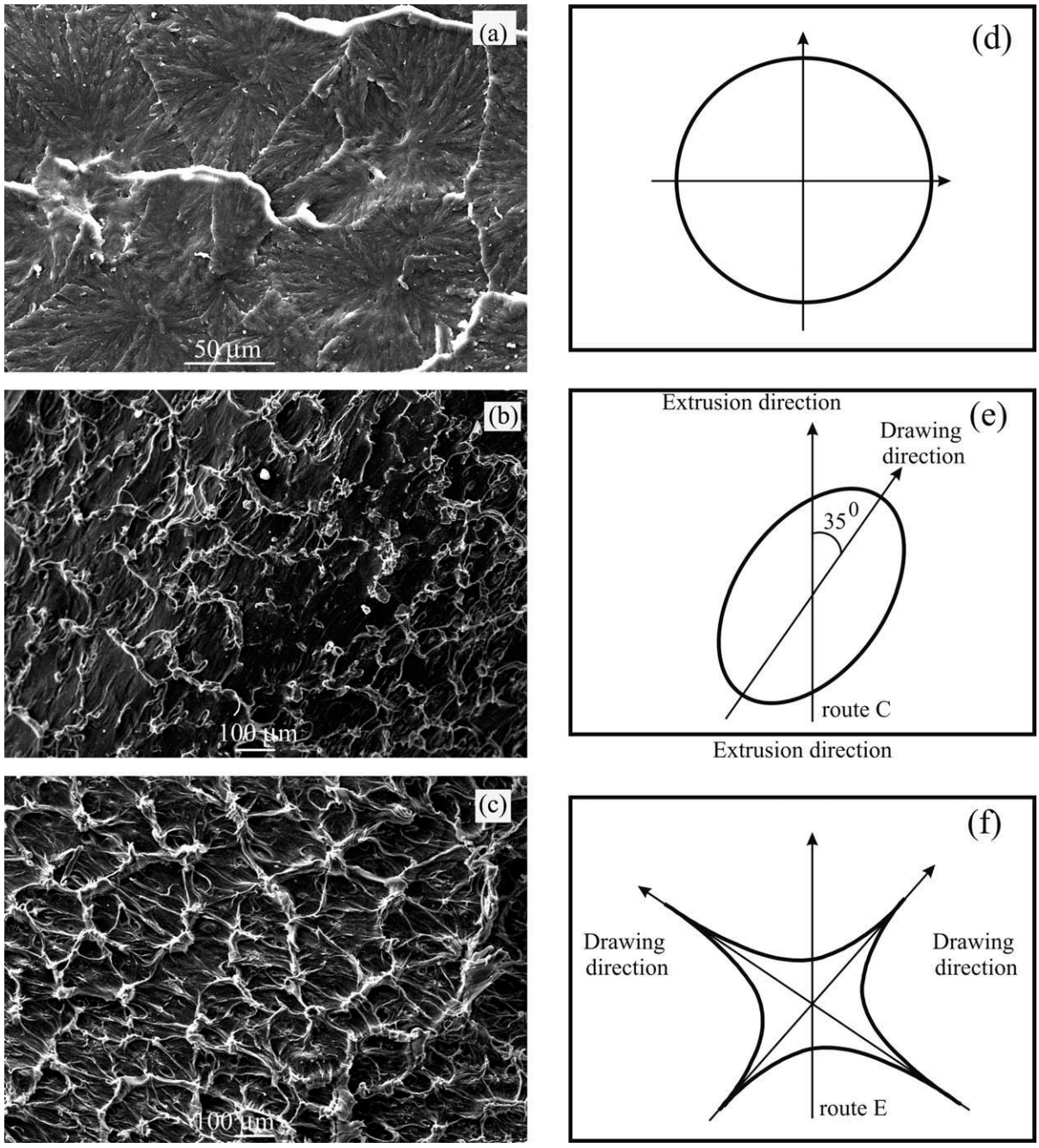

Figure 4. SEM images (a–c) and spherulite transformation schemes of HD1000 (d–f): (a,d)—the initial one; (b,e)—after ECMAE, route C; (d,f)—after ECMAE, route E.

for them in the crystallites. In the case of route C, the level of plastic characteristics is lower, being related to smaller number of interwoven macrofibrils. At the same time, we can observe formation of a lot of tie fibrils are oriented not parallel to the extrusion direction, but almost perpendicular to it (Figure 7), also contributing to conservation of plasticity.

Formation of interwoven macrofibrils as well as their orientation at an angle to extrusion axis determines low anisotropy of microhardness ΔH. The results of structure tests are in agreement with ΔH measurements: the lowest values are achieved along route E, where biaxial orientation of macrofibrils is observed.

Formation of mainly uniaxial oriented structure in the case of route C and biaxial oriented structure at route E is confirmed also by the results of dilatometric analysis. Figure 8 presents elongation $\Delta l/l_0$ of the initial and deformed PE samples at heating. The initial sample behaves as usual within the whole studied temperature region. Its length increases with the temperature rising due to thermal expansion. ECMAE deformation changes the character of $\Delta l/l_0(T)$ dependence. In the case of

Applied Polymer SCIENCE

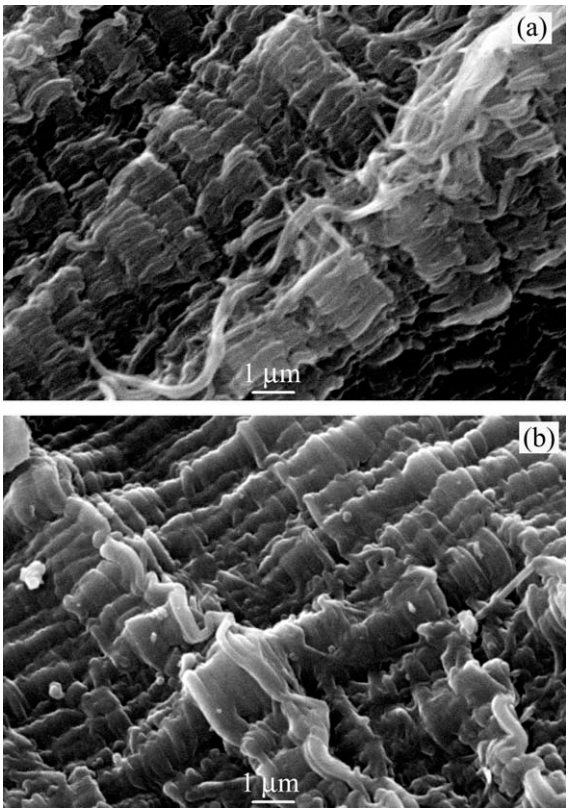

Figure 5. SEM images presenting macrofibrillar structure of HD1000 after different ECMAE routes. (a) route C; (b) route E.

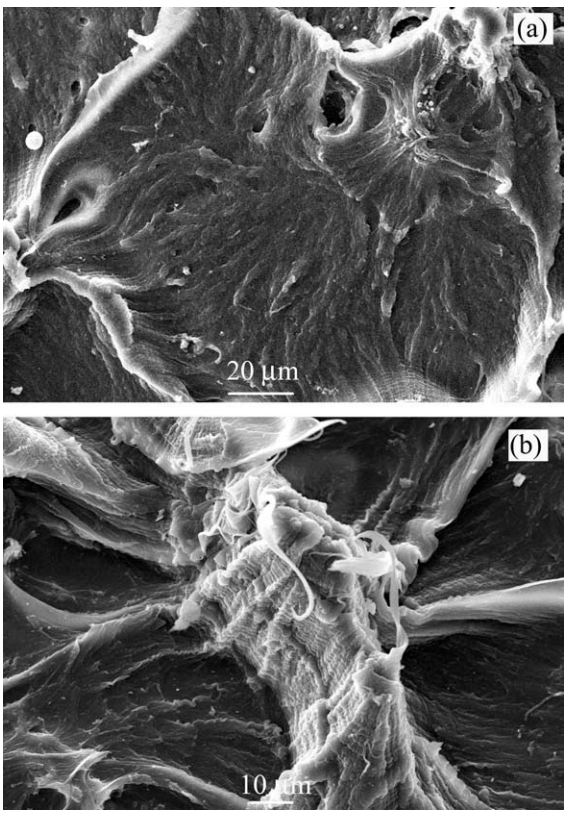

Figure 6. SEM images of spherulite boundaries of HD1000. (a) the initial one, (b) after ECMAE, route E.

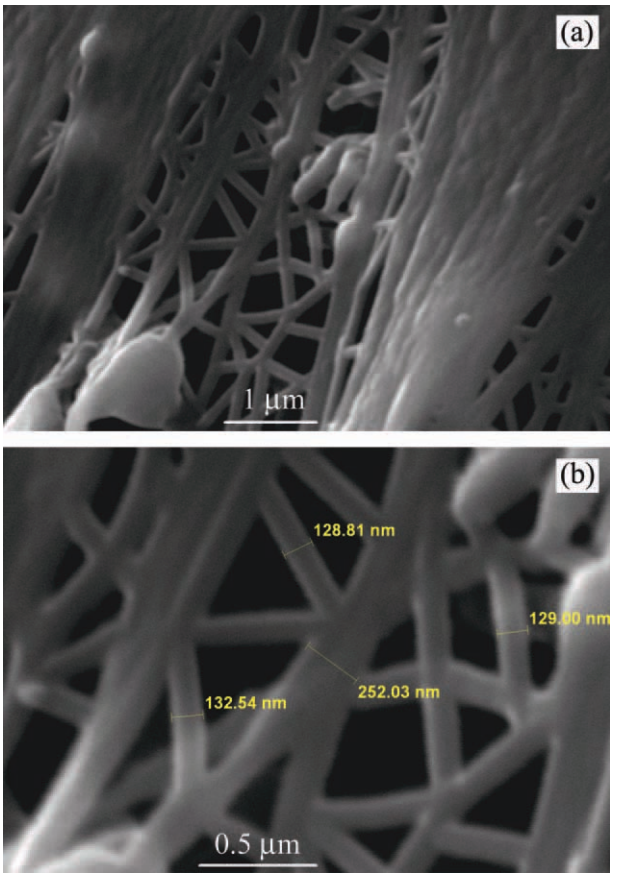

Figure 7. SEM images of tie fibrils of HD1000 after ECMAE, route C.

route C, samples cut from extrudates perpendicular to polymer extrusion direction demonstrated $\Delta l/l_0(T)$ dependence analogous to those of the initial material, and absolute value of $\Delta l/l_0$ increased with heating. The increase of $\Delta l/l_0(T)$ in comparison with undistorted materials was determined by both extrudate

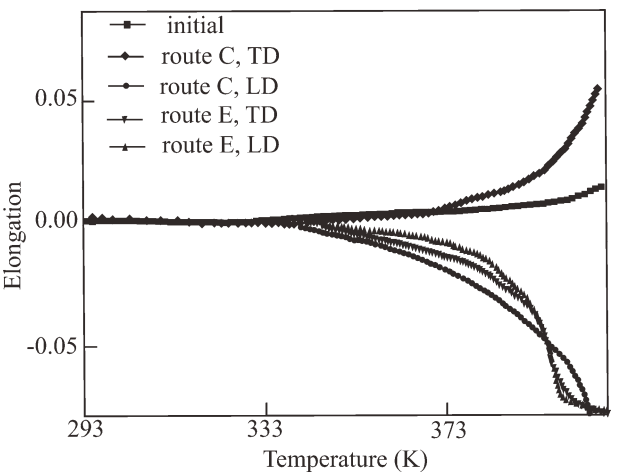

Figure 8. Temperature dependences of the elongation of the initial HD1000 samples and those after ECMAE. TD is the transversal direction, LD is the longitudinal one.

density increase and the presence of compressed amorphous phase located between crystal lamellae. The samples cut across the extrusion direction, $\Delta l/l_0$ was reduced within the whole studied temperature region that was related to the relaxation of the deformed amorphous phase located between crystal lamellae followed by length reduction. The absence of $\Delta l/l_0$ growth until the melting temperatures of extrudates is determined by significant stretching of the amorphous phase, enhanced degree of crystallinity, as well as restraint of amorphous phase relaxation by deformed crystallites.[41]

In the case of route E, the samples cut off both in the longitudinal and transversal direction demonstrated $\Delta l/l_0$ reduced within the whole temperature range. This character of $\Delta l/l_0$ dependence is an evidence of significant stretching of amorphous phase and restrained relaxation of amorphous phase by deformed crystallite in both directions.

Heating up to a temperature of 333 K does not change the value of $\Delta l/l_0$ of the initial PE. After ECMAE along C and E route, these temperatures become 340 and 346K. The increase of the temperature of thermal shrinkage activation can be related to effect of molecular orientation and to the growth of the degree of crystallinity of extrudates.

CONCLUSIONS

The obtained results allow a conclusion that ECMAE is an effective method of solid-phase structure modification of PE that contributes to the set of physical and mechanical properties at conserved high level of plasticity. The main parameters determining effect of ECMAE is deformation intensity, value of accumulated deformation, extrusion rate, and temperature, MM of the polymer and deformation route.

Reduction of polymer MM within the studied region of MM provides higher increase in rigidity and strength, reduced anisotropy of microhardness and yield stress, and conservation of higher level of plasticity. The best set of deformation and strength characteristics, the lowest anisotropy of the properties in longitudinal and transversal directions is observed in the case of route E. The obtained result is related to higher content of crystal phase and degree of crystallite perfection in comparison with route C as well as formation of biaxial-oriented macrofibrillar structure.

ACKNOWLEDGMENTS

The authors express their gratitude to Dr. Burkhovetsky V.V. for assistance when carrying out SEM investigations and to Dr. Grinyov V.G. for UHMWPE samples put at their disposal.

REFERENCES

1. Ward, I. M.; Coates, P. D.; Dumoulin, M. M. Solid Phase Processing of Polymers; Munich: Hanser Gardner, **2000.**
2. Beygelzimer, Y. E.; Beloshenko, V. A. In Encyclopedia of Polymer Science and Technology; Kroschwitz, J. I. Ed.; Wiley: Hoboken, **2004;** Vol. *11*, p 850.
3. Segal, V. M. *Mater. Sci. Eng. Part A* **2004,** *386*, 269.
4. Campbell, B.; Edward, G. *Plast. Rubb. Comp.* **1999,** *28*, 467.
5. Xia, Z.; Hartwig, T.; Sue, H. J. *J. Macromol. Sci. Part B* **2004,** *43*, 385.
6. Ma, J.; Simon, G. P.; Edward, G. H. *Macromolecules* **2008,** *41*, 409.
7. Wang, T.; Tang, S.; Chen, J. *J. Appl. Polym. Sci.* **2011,** *122*, 2146.
8. Sue, H. J.; Li, C. K. Y. *J. Mater. Sci. Lett.* **1998,** *17*, 853.
9. Sue, H. J.; Dilan, H.; Li, C. K. Y. *Polym. Eng. Sci.* **1999,** *39*, 2505.
10. Li, C. K. Y.; Xia, Z. Y.; Sue, H. J. *Polymer* **2000,** *41*, 6285.
11. Xia, Z.; Sue, H. J.; Hsieh, A. J. *J. Appl. Polym. Sci.* **2001,** *79*, 2060.
12. Weon, J. I.; Creasy, T. S.; Sue, H. J.; Hsieh, A. J. *Polym. Eng. Sci.* **2005,** *45*, 314.
13. Creasy, T. S.; Kang, Y. S. *J. Mater. Process. Technol.* **2005,** *160*, 90.
14. Beloshenko, V. A.; Varyukhin, V. N.; Voznyak, A. V.; Voznyak, Yu. V. *Polym. Sci. Ser. A* **2009,** *51*, 1473.
15. Beloshenko, V. A.; Varyukhin, V. N.; Voznyak, A. V.; Voznyak, Yu. V. *Polym. Eng. Sci.* **2010,** *50*, 1000.
16. Beloshenko, V. A.; Voznyak, A. V.; Voznyak, Yu. V. *High Pres. Res.* **2011,** *31*, 153.
17. Beloshenko, V. A.; Varyukhin, V. N.; Voznyak, A. V.; Voznyak, Yu. V. *Polym. Eng. Sci.* **2011,** *51*, 1092.
18. Zachariades, A. E.; Porter, R. S. *J. Appl. Polym. Sci.* **1979,** *24*, 1371.
19. Mead, W. T.; Desper, C. R.; Porter, R. S. *J. Polym. Sci. Part B* **1979,** *17*, 859.
20. Baltá-Calleja, F. J. Structure-Microhardness Correlation of Polymers and Blends; Kluwer: Academic Publishers, **2000.**
21. Flores, A.; Ania, F.; Balta-Calleja, F. J. *Polymer* **2009,** *50*, 729.
22. Crist, B.; Fisher, C. J.; Howard, P. R. *Macromolecules* **1989,** *22*, 1709.
23. Hubert, L.; David, L.; Seguela, R.; Viger, G.; Degoulet, C.; Germain, Y. *Polymer* **2001,** *42*, 8425.
24. Hoffman, J. D. *Polymer* **1982,** *23*, 656.
25. Wunderlich, B.; Czornyj, G. *Macromolecules* **1977,** *10*, 906.
26. Hoffman, J. D.; Miller, R. L. *Polymer* **1997,** *38*, 3151.
27. Xia, Z. Y.; Sue, H. J.; Rieker, T. P. *Macromolecules* **2000,** *33*, 8746.
28. Aour, B.; Zairi, F.; Nait-Abdelaziz, M.; Gloagnen, J. M.; Lefebvre, J. M. *Key Eng. Mater.* **2010,** *424*, 71.
29. Thomas, L. S.; Cleereman, K. J. *SPE J.* **1972,** *28*, 61.
30. Chun, B. K.; Jinn, J. T.; Lee, J. K. *Intern. J. Plast.* **2002,** *18*, 571.
31. Hope, P. S.; Gibson A. G.; Ward, I. M. *J. Polym. Sci. Part B* **1980,** *18*, 1243.
32. Mohanraj, J.; Bonner, M. J.; Barton, D. C.; Ward, I. M. *Polymer* **2006,** *47*, 5897.

33. Mohanraj, J.; Morawiec, J.; Pawlak, A.; Barton, D. C.; Galeski, A.; Ward, I. M. *Polymer* **2008,** *49*, 303.

34. Ivankova, E.; Vasilieva, V.; Myasnikova, L.; Marikhin, V.; Henning, S.; Michler, G. H. *e-Polymers* **2002,** *44*, 1.

35. Dubnikova, I. L.; Petrosyan, A. I.; Topolkaraev, V. A.; Tovmasyan, Yu, M.; Meshkova, I. N.; D'yachkovskii, F. S. *Polym. Sci. Ser. A* **1988,** *30*, 2345.

36. Bartczak, Z.; Morawiec, J.; Galeski, A. *J. Appl. Polym. Sci.* **2002,** *86*, 1413.

37. Kozlov, H. V.; Beloshenko, V. A.; Aloiev, V. Z.; Varyukhin, V. N. *Mater. Sci.* **2000,** *36*, 98.

38. Zhorin, V. A.; Kiselev, M. R.; Roldugin, V. I. *Polym. Sci. Ser. B* **2001,** *43*, 1262.

39. Chen, X.; Galeski, A.; Michler, G. H. *Polymer* **2006,** *47*, 3171.

40. Bartczak, Z.; Kozaneski, M. *Polymer* **2005,** *46*, 8210.

41. Salamatina, O. B.; Rudnev, S. N.; Bartczak, Z.; Galeski, A.; Oleinik, E. F. *Polym. Sci. Ser. A* **2011,** *53*, 775.